J|A|C|S
ARTICLES
Published on Web 11/18/2006

Proton-Shuffle Mechanism of O−O Activation for Formation of a High-Valent Oxo−Iron Species of Bleomycin

Devesh Kumar,[†] Hajime Hirao,[†] Sason Shaik,*[,†] and Pawel M. Kozlowski*[,†,‡,§]

Contribution from the Department of Organic Chemistry and the Lise Meitner-Minerva Center for Computational Quantum Chemistry, The Hebrew University, Jerusalem 91904, Israel, and Department of Chemistry, University of Louisville, Louisville, Kentucky 40292

Received June 29, 2006; E-mail: sason@yfaat.ch.huji.ac.il; pawel@louisville.edu

Abstract: Bleomycins (BLMs) can utilize H_2O_2 to cleave DNA in the presence of ferric ions. DFT calculations were used to study the mechanism of O−O bond cleavage in the low-spin Fe^{III}−hydroperoxo complex of BLM. The following alternative hypotheses were investigated using realistic structural models: (a) heterolytic cleavage of the O−O bond, generating a Compound I (Cpd I) like intermediate, formally BLM−Fe^{V}═O; (b) homolytic O−O cleavage, leading to a BLM−Fe^{IV}═O species and an OH• radical; and (c) a direct O−O cleavage/H-abstraction mechanism by ABLM. The calculations showed that (a) is a facile and viable mechanism; it involves acid−base proton reshuffle mediated by the side-chain linkers of BLM, causing thereby heterolytic cleavage of the O−O bond and generation of Cpd I. Formation of Cpd I is found to involve a barrier of 13.3 kcal/mol, which is lower than the barriers in the alternative mechanisms (b and c) that possess respective barriers of 31 and 17 kcal/mol. The so-formed Cpd I species with a radical on the side-chain linker, methylvalerate (**V**), adjacent to the BLM−Fe^{IV}═O complex, resembles the formation of the active species of cytochrome *c* peroxidase in the Poulos−Kraut proton-shuffle mechanism in heme peroxidases (Poulos, T. L.; Kraut, J. *J. Biol. Chem.* **1980**, *255*, 8199−8205). Experimental data are discussed and shown to be in accord with this proposal. It suggests that the high-valence Cpd I species of BLM participates in the DNA cleavage. This is an alternative mechanistic hypothesis to the exclusive reactivity scenario based on ABLM (Fe^{III}−OOH).

Introduction

In the past few years the bioinorganic community has gained growing understanding of the action of mononuclear non-heme iron enzymes[1−5] that utilize dioxygen to catalyze a variety of biological reactions. It is generally held now[2,4] that the oxidative transformations performed by these non-heme iron enzymes involve ferryl intermediates having high-valent oxoiron(IV) and sometimes perferryl oxoiron(V) species. Such intermediates were directly observed in enzymatic[5,6] and biomimetic[7−11] reactions; some model complexes have even been characterized by X-ray crystallography.[7,11] Furthermore, methods of computational chemistry have been applied to elucidate the electronic and structural properties as well as the reactivity patterns of these and analogous non-heme species.[12−17] Since the oxoiron species appears to be a generally viable intermediate with high reactivity, it is important to inquire about the existence of these species in other non-heme systems. Accordingly, the present study focuses on the non-heme iron complex of bleomycin (BLM) and seeks a low-energy path for generating high-valent iron intermediates in this unusual peptide.

Bleomycins ($BLM(H_2)$; see Figure 1) form a group of glycopeptide antibiotics that are used in the treatment of

[†] The Hebrew University.
[‡] University of Louisville.
[§] Fulbright Visiting Professor under the United States−Israeli Educational Foundation (USIEF).

(1) Costas, M.; Mehn, M. P.; Jensen, M. P.; Que, L., Jr. *Chem. Rev.* **2004**, *104*, 939−986.
(2) Shan, X.; Que, L., Jr. *J. Inorg. Biochem.* **2006**, *100*, 421−433.
(3) Solomon, E. I.; Brunold, T. C.; Davis, M. I.; Kemsley, J. N.; Lee, S. K.; Lehnert, N.; Neese, F.; Skulan, A. J.; Yang, Y. S.; Zhou, J. *Chem. Rev.* **2000**, *100*, 235−349.
(4) Groves, J. T. *J. Inorg. Biochem.* **2006**, *100*, 434−447.
(5) Price, J. C.; Barr, E. W.; Tirupati, B.; Bollinger, J. M., Jr.; Krebs, C. *Biochemistry* **2003**, *42*, 7497−7508.
(6) Proshlyakov, D. A.; Henshaw, T. F.; Monterosso, G. R.; Ryle, M. J.; Hausinger, R. P. *J. Am. Chem. Soc.* **2004**, *126*, 1022−1023.
(7) Rohde, J.-U.; In, J.-H.; Lim, M. H.; Brennessel, W. W.; Bukowski, M. R.; Stubna, A.; Münck, E.; Nam, W.; Que, L., Jr. *Science* **2003**, *299*, 1037−1039.
(8) Lim, M. H.; Rohde, J.-U.; Stubna, A.; Bukowski, M. R.; Costas, M.; Ho, R. Y. N.; Münck, E.; Nam, W.; Que, L., Jr. *Proc. Natl. Acad. Sci. U.S.A.* **2003**, *100*, 3665−3670.
(9) Rohde, J.-U.; Torelli, S.; Shan, X.; Lim, M. H.; Klinker, E. J.; Kaizer, J.; Chen, K.; Nam, W.; Que, L., Jr. *J. Am. Chem. Soc.* **2004**, *126*, 16750−16761.
(10) Kaizer, J.; Klinker, E. J.; Oh, N. Y.; Rohde, J.-U.; Song, W. J.; Stubna, A.; Kim, J.; Münck, E.; Nam, W.; Que, L., Jr. *J. Am. Chem. Soc.* **2004**, *126*, 472−473.
(11) Bukowski, M. R.; Koehntop, K. D.; Stubna, A.; Bominaar, E. L.; Halfen, J. A.; Münck, E.; Nam, W.; Que, L., Jr. *Science* **2005**, *310*, 1000−1002.
(12) Bassan, A.; Blomberg, M. R. A.; Siegbahn, P. E. M. *Chem. Eur. J.* **2003**, *9*, 4055−4067.
(13) Bassan, A.; Blomberg, M. R. A.; Siegbahn, P. E. M.; Que, L., Jr. *Chem. Eur. J.* **2005**, *11*, 692−705.
(14) Quiñonero, D.; Morokuma, K.; Musaev, D. G.; Mas-Ballesté, R.; Que, L., Jr. *J. Am. Chem. Soc.* **2005**, *127*, 6548−6549.
(15) (a) Kumar, D.; Hirao, H.; Que, L., Jr.; Shaik, S. *J. Am. Chem. Soc.* **2005**, *127*, 8026−8027. (b) Hirao, H.; Kumar, D.; Que, L., Jr.; Shaik, S. *J. Am. Chem. Soc.* **2006**, *128*, 8590−8606.
(16) Decker, A.; Solomon, E. I. *Angew. Chem., Int. Ed.* **2005**, *44*, 2252−2255.
(17) Buda, F.; Ensing, B; Grinbau, M. C. M.; Baerends, E. J. *Chem. Eur. J.* **2001**, *7*, 2775−2783. (b) Ensing, B.; Buda, F.; Gribnau, M. C. M.; Baerends, E. J. *J. Am. Chem. Soc.* **2004**, *126*, 4355−4365.

10.1021/ja064611o CCC: $33.50

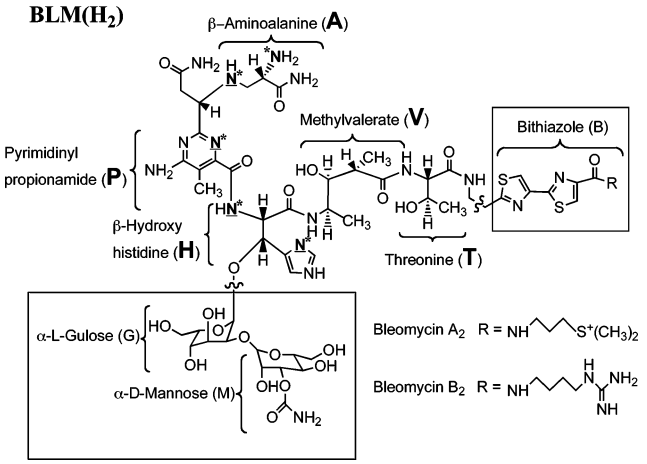

Figure 1. Representation of bleomycin ($BLM(H_2)$); the parenthetical H_2 signifies the neutral molecule with two protons on the secondary NH groups in the side chains **A** and **H**. The asterisks on the nitrogen atoms indicate coordination sites to the iron. Boxed fragments were deleted and replaced by hydrogen atoms in DFT calculations (see later).

carcinomas and lymphomas.[18] The activity of the drug is thought to derive from its ability to degrade double-stranded DNA.[19−22] DNA degradation is both oxygen and metal-ion dependent, with the greatest enhancement observed in vivo for iron. The initial species is believed to be $BLM-Fe^{II}$ that binds O_2 to produce formally a Fe^{III}−superoxide complex that accepts an additional electron and forms the low-spin end-on Fe^{III}−hydroperoxide complex ($Fe^{III}-OOH$), referred to as the "activated" bleomycin (ABLM).[23−25] Alternatively, a spectroscopically identical ABLM can be generated by a reaction of $BLM-Fe^{III}$ with H_2O_2.

While $Fe^{III}-OOH$ is certainly a key intermediate in the cycle of belomycin,[25−27] doubts still exist whether this hydroperoxo complex of iron bleomycin is indeed the final active species that interacts with DNA via direct hydrogen abstraction or whether the mechanism involves homolytic or heterolytic O−OH bond cleavage leading to high-valence ferryl, $Fe^{IV}=O$, and an OH radical or a perferryl $Fe^{V}=O$ species (see later; this species is actually $Fe^{IV}=O/\mathbf{V}^{+\bullet}$; **V** being methylvalerate**)**, which are responsible for initiating DNA strand scission (see Figure 2 for details).

All three mechanisms, in Figure 2, have been suggested based on different experimental observations. The ABLM (Figure 2) hypothesis rests on the experimental facts that $Fe^{III}OOH$ is the last detectable intermediate,[28] that the observed ^{18}O kinetic isotope effect (KIE) was argued to fit better O−O cleavage of a peroxide species than an $Fe^{IV}=O$ cleavage,[29] and that the

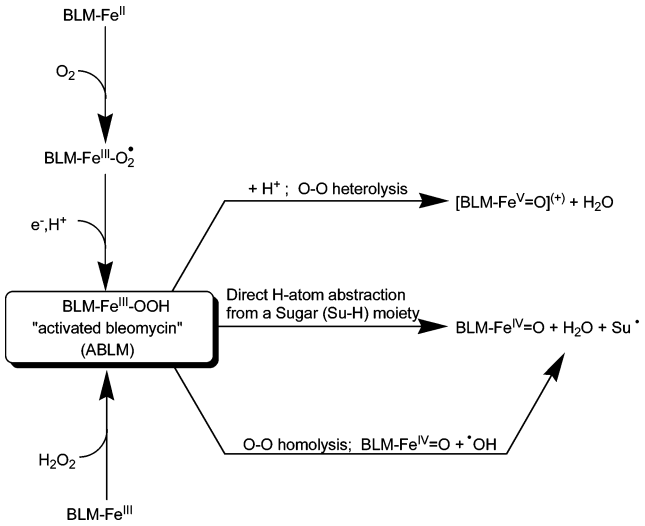

Figure 2. Mechanistic hypotheses of O−O bond cleavages in ABLM.

Mössbauer and EPR parameters show $Fe^{III}-OOH$ but not $Fe^{IV}=O$.[30] Studies based on the reaction of $Fe^{III}-BLM$ with 10-hydroperoxy-8,12-octadecadienoic acid and analysis of the reduction products revealed the operation of a major homolytic cleavage path[31] of the O−O bond to form a $BLM-Fe^{IV}=O$ intermediate (Figure 2) along with a minor heterolytic cleavage path. Finally, since many of the reactivity patterns of BLM resemble those of cytochromes P450 (P450), the presence of a putative $BLM-Fe^{V}=O$ intermediate has been also proposed,[32,33] by analogy to the heme-based Compound I (Cpd I).[34] KIE(H/D) studies of the DNA cleavage led to values of 2−7.[35] Thus, while these KIE(H/D) results, especially at the high end, seem to rule out participation of a hydroxyl ($OH^{\bullet}$) radical in H abstraction, the significant KIE(H/D) values may fit either H abstraction by a perferryl species or directly[27] by the Fe−OOH species.

The conundrum of $Fe^{III}-OOH$ or $Fe^{IV}=O/Fe^{V}=O$ in the field of bleomycin is similar to the mechanistic debates concerning the activity of P450s[4,36−42] and the intriguing controversy whether or not an iron(III)−hydroperoxo species is involved as a "second electrophilic oxidant" in oxygenation reactions of these enzymes. A very similar dichotomy exists for non-heme

(18) Umezawa, H. In *Bleomycin*; Hecht, S. M., Ed., Springer-Verlag: New York, 1979; pp 24−36.
(19) Stubbe, J.; Kozarich, J. *Chem. Rev.* **1987**, *87*, 1107−1136.
(20) Stubbe, J.; Kozarich, J. W.; We, W.; Vanderwall, D. E. *Acc. Chem. Res.* **1996**, *29*, 322−330.
(21) Claussen, C. A.; Long, E. C. *Chem. Rev.* **1999**, *99*, 2797−2816.
(22) Chen, J.; Stubbe, J. *Curr. Opin. Chem. Biol.* **2004**, *8*, 175−181.
(23) Burger, R. M.; Peisach, J.; Horwitz, S. B. *J. Biol. Chem.* **1981**, *256*, 11636−11644.
(24) Burger, R. M.; Kent, T. A.; Horwitz, S. B.; Münck, E.; Peisach, J. *J. Biol. Chem.* **1983**, *258*, 1559−1564.
(25) Neese, F.; Zaleski, J. F.; Zaleski, K. L.; Solomon, E. I. *J. Am. Chem. Soc.* **2000**, *122*, 11703- 11724.
(26) Lehnert, N.; Neese, F.; Ho, R. Y.; Que, L., Jr. *J. Am. Chem. Soc.* **2002**, *124*, 10810−10822.
(27) Solomon, E. I.; Decker, A.; Lehnert, N. *Proc. Natl. Acad. Sci.* **2003**, *100*, 3589−3594.
(28) Sam, J. W.; Tang, X. J.; Peisach, J. *J. Am. Chem. Soc.* **1994**, *116*, 5250−5256.
(29) Burger, R. M.; Tian, G.; Drilca, K. *J. Am. Chem. Soc.* **1995**, *117*, 1167−1168.
(30) Peisach, J. *Int. Congress Ser.* **2002**, *1233*, 511−517.
(31) Padbury, G.; Sligar, S. G.; Labeque, R.; Marnett, L. J. *Biochemistry* **1988**, *27*, 7846−7852.
(32) Hecht, S. M. *J. Nat. Prod.* **2000**, *63*, 158−168.
(33) Parvital, G.; Bernadou, J.; Meunier, B. *Biochem. Pharmacol.* **1989**, *38*, 133−140.
(34) Harris, D. L. *Curr. Opin. Chem. Biol.* **2001**, *5*, 724−735.
(35) Worth, L., Jr.; Frank, B. L.; Christner, D. F.; Absalon, M. J.; Stubbe, J.; Kozarich, J. W. *Biochem*istry **1993**, *32*, 2601−2609.
(36) In *Cytochrome P450: Structure, Mechanism and Biochemistry*, 2nd ed.; Ortiz de Montellano, P. R., Ed.; Plenum Press: New York, 1995.
(37) Denisov, I. G.; Makris, T. M.; Sligar, S. G.; Schlichting, I. *Chem. Rev.* **2005**, *105*, 2253−2278.
(38) In *Cytochrome P450: Structure, Mechanism and Biochemistry*, 3rd ed.; Ortiz de Montellano, P. R., Ed.; Kluwer Academic/Plenum Publishers: New York, 2004.
(39) (a) Ogliaro, F.; de Visser, S. P.; Cohen, S.; Sharma, P. K.; Shaik, S. *J. Am. Chem. Soc.* **2002**, *124*, 2806−2817. (b) Sharma, P. K.; de Visser, S. P.; Shaik, S. *J. Am. Chem. Soc.* **2003**, *125*, 8698−8699. (c) Kamachi, T.; Shiota, Y.; Ohta, T.; Yoshizawa, K. *Bull Chem. Soc. Jpn.* **2003**, *76*, 721−732. (d) Derat, E.; Kumar, D.; Hirao, H.; Shaik, S. *J. Am. Chem. Soc.* **2006**, *128*, 473−484.
(40) Jin, S.; Bryson, T. A.; Dawson, J. H. *J. Biol. Inorg. Chem.* **2004**, *9*, 644−653.
(41) Nam, W.; Ryu, Y. O.; Song, W. J. *J. Biol. Inorg. Chem.* **2004**, *9*, 654−660.
(42) Shaik, S.; de Visser, S. P.; Kumar, D. *J. Biol. Inorg. Chem.* **2004**, *9*, 661−668.

iron enzymes and their model compounds.[2,4,27,43,44] In the case of P450, the Fe═O species is known to exist[4] but has not been observed in a working cycle, whereas the $Fe^{III}OOH$ species was observed as the last station before the appearance of the monooxygenation product (5-hydroxycamphor in $P450_{cam}$).[37] Nevertheless, the $Fe^{III}OOH$ complex was shown to be a sluggish oxidant (compared with Cpd I) by both theory[39] and experiment.[40] Similarly, in the non-heme area too it was shown, just this year, that the $Fe^{III}-OOH$ species is a sluggish oxidant compared with $Fe^{IV}═O$.[43] This sluggishness in addition to the general observation that the reactivity of Fe−OOH species, even when positively charged, requires acid calyalysis[4] are compelling enough to initiate a search for an alternative hypothesis.

Clearly, therefore, the fact that the ferryl species has not been observed in bleomycin cannot be taken as a definitive proof that DNA cleavage is dominated by $Fe^{III}-OOH$ (ABLM). In fact, despite the arguments in favor of ABLM and against the ferryl/perferrryl hypotheses (see Figure 2),[25−27] the evidence behind the arguments is largely indirect and inconclusive. For example, a recent argument[30] that bleomycin acts as an oxidase and is therefore different than P450[30] is not necessarily decisive evidence since perferryl species can certainly act as oxidases and lead also to related desaturation reactions.[45] Another example is the KIE(^{18}O) value observed during the decay of activated BLM and used for assigning the decaying species as the $Fe^{III}-OOH$ species.[29] Thus, the mechanism leading to the observed KIE(^{18}O) value (1.054) was assessed relative to estimated equilibrium isotope effect (EIE) data for a few possible processes. These EIE data were evaluated based on a combination of known and some estimated frequencies from a variety of model compounds and used to rule out the decay of a ferryl/perferryl species and support the decay of a $Fe^{III}-OOH$ species. However, considering the uncertainty of the data, the observed KIE(^{18}O) could as well fit the involvement of a Fe═O species. As we argue here later, the observed KIE(^{18}O) may in fact correspond to formation of Cpd I by O−O activation. Finally, the past tendency[28−30] to rule out a Fe═O species because it could not be detected and because "high-valent intermediates were not observed in non-heme systems" is no longer tenable since these species appear now in non-heme catalysts[2,4,7,11] and in the TauD enzyme.[5,6] In this sense, it is perhaps essential to reiterate the recent demonstration of Nam and co-workers that non-heme iron(III)−hydroperoxo species are sluggish oxidants and that the oxidizing power of the intermediates cannot compete with that of high-valent iron(IV)−oxo complexes.[43] This direct evidence forms a strong incentive to explore a low-energy mechanism for the formation of the $Fe^{V}O$ species in bleomycin.

Following this incentive, the present study uses density functional theory (DFT) to investigate heterolytic modes of O−O bond cleavage of a $BLM-Fe^{III}-H_2O_2$ complex. As this investigation reveals, there exist low-energy mechanisms that are mediated by the side chains (**T** and/or **V**, in Figure 1) of BLM and lead to formation of high-valence iron−oxo species. The BLM side chains promote proton reshuffle and lead thereby to O−O bond heterolysis with small barriers and in a manner reminiscent of the Poulos−Kraut mechanism in peroxidases.[46−48] Thus, a Cpd I like species may be energetically accessible in bleomycin. We think that this prediction offers an alternative hypothesis, reopens the field, and forms a basis for the interplay between theory and experiment.

Methods

DFT calculations were carried out for the mechanisms in Figure 2. Geometry optimization was performed with the B3LYP[49] functional using JAGUAR 5.5.[50] Two basis sets were employed: LACVP* (B1, LACVP(Fe)/6-31G*(rest))[51] was applied for geometry optimization, while the larger one LACV3P++** (B2, LACV3P + a diffuse d function(Fe)/6-311++G**(rest)), was used for single-point energy evaluation. Since bleomycin functions in aqueous solution, the relative energies of all the structures were corrected using the solvent model implemented in JAGUAR 5.5 (the program defines the solvent by its dielectric constant, ϵ, and probe radius, r; for water, $\epsilon = 80.4$ and $r = 1.40$ Å). Due to the very large size of the system, we performed frequency calculation only for TS_{O-O}, the highest energy species in the heterolytic mechanisms (see Figures 6 and 7 later). The frequency calculation was done with GAUSSIAN 03.[52] Many other calculations were carried out for various models of ABLM. The data generated by the study are collected in the Supporting Information.

Results

1. Structure of $Fe^{III}-OOH$ Complexes of Bleomycin. Computational modeling[53,54] of high-spin ferrous $BLM-Fe^{II}$ or ferric $BLM-Fe^{III}$ complexes, precursors of ABLM, is computationally challenging because there is no crystal structure available and the nature of the axial ligands is uncertain. There are several synthetic models where BLM serves as a ligand and which were crystallized with various metals, for example, copper, cobalt, zinc, and even iron.[21] All of these complexes lack both the bithiazole and the sugar moieties (Figure 1). Most of the knowledge available on the structure of various metallo-BLM complexes in solution is derived from spectroscopic data and studies combining multinuclear NMR experiments and molecular dynamics simulations.[55,56] The same applies to the $BLM-Fe^{III}-$hydroperoxide complex (ABLM), which was the initial target of our investigation. To construct a realistic model of the ABLM, the 2D-NMR spectroscopic structure (PDB IGJ2, see Figure 3a) of $BLM-Co^{III}-OOH$ bound to the 3′-PG lesion was used as a basis of our study.[57] The initial Cartesian

(43) Park, M. J.; Lee, J.; Suh, Y.; Kim, J.; Nam, W. *J. Am. Chem. Soc.* **2006**, *128*, 2630−2634.
(44) Que, L., Jr. *J. Biol. Inorg. Chem.* **2004**, *9*, 684−690.
(45) (a) Kumar, D.; de Visser, S. P.; Shaik, S. *J. Am. Chem. Soc.* **2004**, *126*, 5072−5073. (b) Mueller, E.J.; Lioda, P. J.; Sligar, S. G. Twenty-five Years of $P450_{cam}$ Research: Mechanistic Insights into Oxygenase Catalysis. In *Cytochrome P450: Structure, Mechanism and Biochemistry*, 2nd ed.; Ortiz de Montellano, P. R., Ed.; Plenum Press: New York, 1995; pp 83−124. (c) Hackett, J. C.; Brueggemeier, R. W.; Hadad, C. M. *J. Am. Chem. Soc.* **2005**, *127*, 5224−5237.
(46) Poulos, T. L. Peroxidases and Cytochrome P450. In *The Porphyrin Handbook*; Kadish, K. M., Smith, K. M., Guilard, R., Eds.; Academic Press: New York, 2000; Vol. 4, Chapter 32, pp 189−218.
(47) Poulos, T. L.; Kraut, J. *J. Biol. Chem.* **1980**, *255*, 8199−8205.
(48) Derat, E.; Shaik, S. *J. Phys. Chem. B* **2006**, *110*, 10526−10533.
(49) (a) Becke, A. D. *J. Chem. Phys.* **1992**, *96*, 2155−2160. (b) Becke, A. D. *J. Chem. Phys.* **1992**, *97*, 9173−9177. (c) Becke, A. D. *J. Chem. Phys.* **1993**, *98*, 5648−5652. (d) Lee, C.; Yang, W.; Parr, R. G. *Phys. Rev. B* **1988**, *37*,785−789.
(50) *JAGUAR 5.5*; Schrodinger, Inc.: Portland, OR, 2004.
(51) The LACVP family of basis sets is derived from LANDL2DZ, see: (a) Hay, J. P.; Wadt, W. R. *J. Chem. Phys.* **1985**, *82*, 299−310. (b) Friesner, R. A.; Murphy, R. B.; Beachy, M. D.; Ringnalda, M. N.; Pollard, W. T.; Dunietz, B. D.; Cao, Y. *J. Phys. Chem. A* **1999**, *103*, 1913−1928.
(52) Frisch, M. J. et al. *Gaussian 03*; Gaussian, Inc.: Wallingford CT, 2004.
(53) Freindorf, M.; Kozlowski, P. M. *J. Phys. Chem. A* **2001**, *105*, 7267−7272.
(54) Karawajczyk, A.; Buda, F. *J. Biol. Inorg. Chem.* **2005**, *10*, 33−40; Errata *J. Biol. Inorg. Chem.* **2005**, *10*, 208.
(55) Lehman, T. E.; Serrano, M. L.; Que, L. *Biochemistry* **2000**, *39*, 3886−3898.
(56) Lehman, T. E. *J. Biol. Inorg. Chem.* **2002**, *7*, 305−312.
(57) Hoehn, S. T.; Junker, H.-D.; Bunt, R. C.; Turner, C. J.; Stubbe, J. *Biochemistry* **2001**, *40*, 5894−5905.

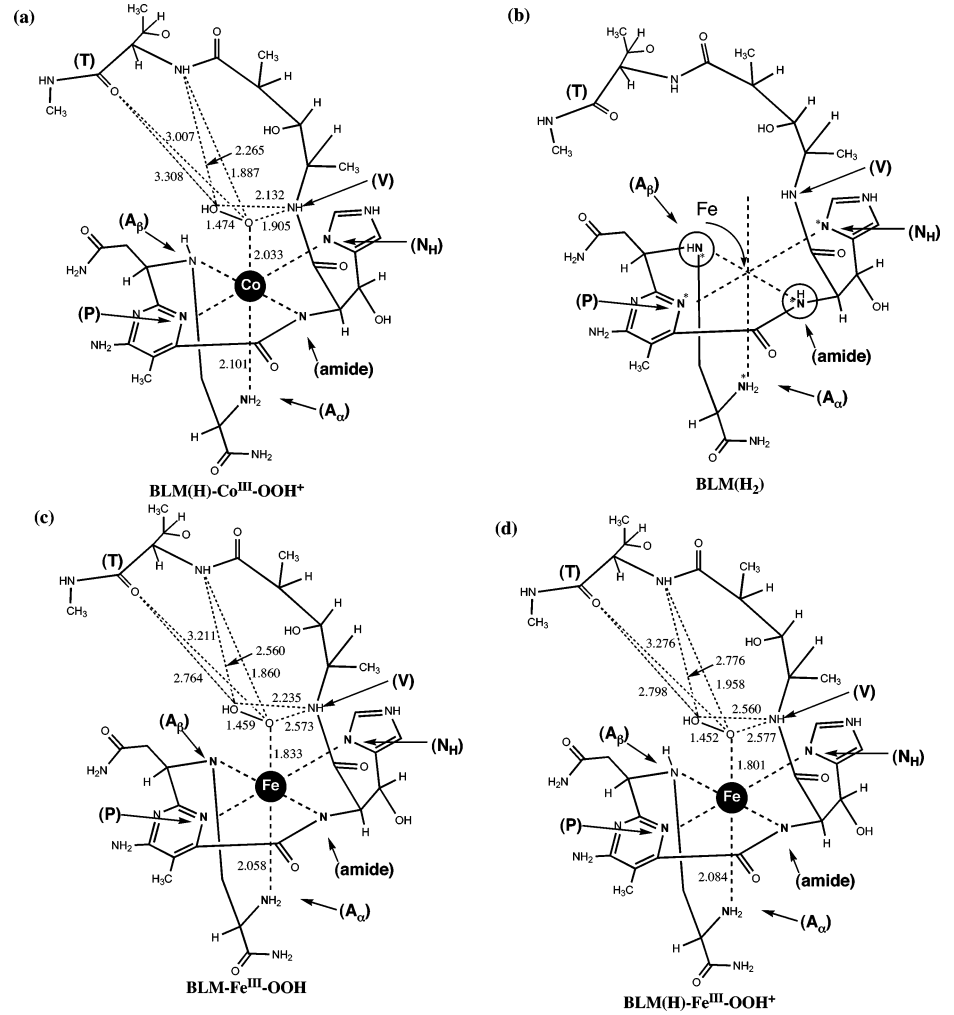

Figure 3. (a) Experimental structure of BLM(H)−Co^{III}−OOH determined by 2D NMR spectroscopy from ref 57. (b) The truncated neutral ligand BLM-(H_2). Parts c and d show DFT (UB3LYP/B1) optimized structures of ^{2}BLM−Fe^{III}−OOH and ^{2}BLM(H)−Fe^{III}−OOH$^+$. Group labels follow Figure 1.

coordinates were extracted from the file, and the cobalt atom was replaced by iron (Figure 3b). The iron-substituted structure was simplified by cutting off the gulose, mannose, and bithiazole moieties (boxed parts in Figure 1) while capping the dangling bonds by hydrogen atoms. The truncated ligand is depicted in Figure 3b and labeled as BLM(H_2), and in this state it is neutral; the five nitrogen moieties that serve as ligands are indicated with asterisks.

For the ferric complexes we considered two different protonation states of the ligand, as shown in Figure 3c and 3d. In the first case (Figure 3c) two protons were removed from the NH(amide) and NH(**A**$_\beta$) groups to create a neutral BLM−Fe^{III}−OOH complex; here the bleomycin ligand is BLM^{2-}. In the second case (Figure 3d) only the NH(amide) group was deprotonated to generate a cationic BLM(H)−Fe^{III}−OOH$^+$ complex; here the ligand is BLM(H)$^{1-}$ (note: a third candidate of BLM(H)−Fe^{III}−OOH$^+$ with a deprotonated NH(**A**$_\beta$) and protonated N(amide) groups was not considered here). The geometries of the so-constructed model complexes were optimized for the doublet and quartet spin states. Since the doublet spin state was confirmed as the ground state of both BLM−Fe^{III}−OOH and BLM(H)−Fe^{III}−OOH$^+$, only the geometries for the doublet state complexes are shown in Figure 3c and 3d.

As expected, the impact of the protonation states of the amide groups on the Fe−N and Fe−O bond lengths is marginal. The geometric parameters for both optimized models are similar to the ones reported for the structure based on 2D-NMR data (Figure 3a vs 3c and 3d).[57] The predicted changes of axial Fe−O and Fe−N bond lengths are consistent with replacement of the cobalt by iron, and the orientations of the Fe−OOH and Co−OOH moieties are similar. In the three complexes the side chains donate hydrogen bonds to the OOH moiety; one is donated by the NH(**V**) group of the side-chain methylvalerate (**V**) moiety and the other by the NH(**T**) moiety of the threonine (**T**) side chain. Thus, the absence of DNA, in the calculations, does not significantly alter the topology of the M−OOH moiety. This finding is consistent with the recent resonance Raman demonstration that the isotope ^{16}O/^{18}O difference spectrum is essentially identical for the free and the DNA-bound BLM(H)−Co^{III}−OOH$^+$ complexes.[58] The other issue is the chirality of ABLM, which was recently analyzed by Stubbe.[22] The chirality of our model based on the Stubbe structure[57] is also consistent with the structure of the copper complex, corresponding to BLM−Cu^{II}−Cl bound to resistance protein, published by Sugiyama (PDB code 1JIF).[59] Furthermore, recent DFT analysis of the interligand vibrations of Co−OOH in BLM−Co^{III}−OOH

(58) Rajani, C.; Kincaid, J. R.; Petering, D. H. *J. Am. Chem. Soc.* **2004**, *126*, 3829−3836.
(59) Sugiyama, M.; Kumagai, T.; Hayashida, M.; Maruyama, M.; Matoba, Y. *J. Biol. Chem.* **2002**, *277*, 2311−2320.

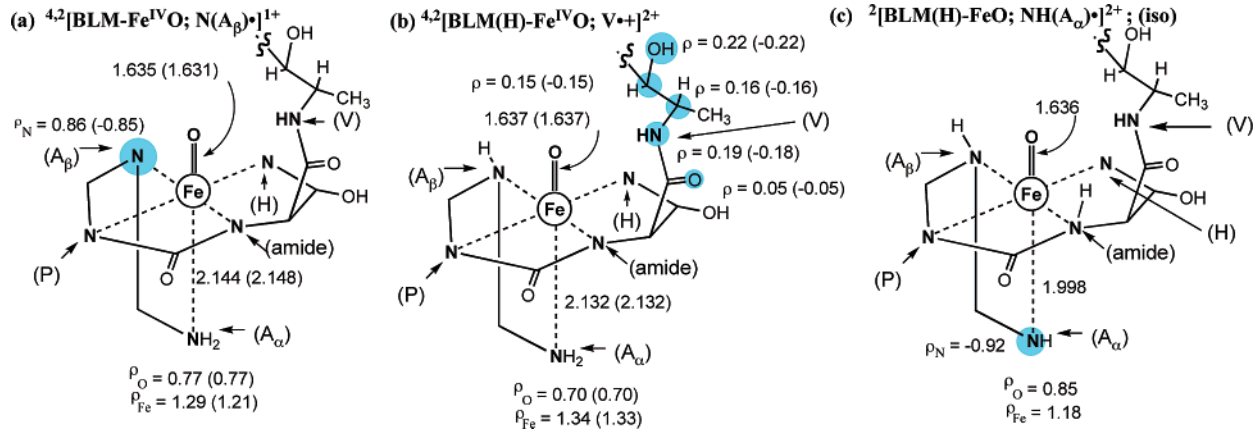

Figure 4. Structures of BLM analogues of Cpd I, generated from the ABLMs of Figure 3c and 3d. The structures are drawn in a truncated manner for the sake of clarity. Spin density distribution (values labeled as ρ) is highlighted. The set of two values correspond to the ferromagnetic (antiferromagnetic) spin states with $S = 3/2$ ($S = 1/2$). (a) The $[^{2,4}$BLM$-$Fe^{IV}=O;N(**A**$_\beta$)$^\bullet]^+$ species. (b) The $[^{2,4}$BLM(H)$-$Fe^{IV}=O;**V**$^{\bullet+}]^{2+}$ species, where the **A**$_\beta$ amide is protonated, i.e., NH(**A**$_\beta$). (c) The isomer species of the one shown in Figure 4b: the $[^{2,4}$BLM(H)$-$Fe^{IV}=O;NH(**A**$_\alpha$)$^\bullet]^{2+}$ (iso) species with protonated NH(**amide**) and NH(**A**$_\beta$) groups and a deprotonated NH (**A**$_\alpha$) group.

have demonstrated that only this model is in fact consistent with ^{16}O/^{18}O isotope-sensitive modes present in the Raman spectrum.[60]

Thus, all in all, these results indicate that both structural models of ABLM are appropriate for studies of the O$-$O bond cleavage in the next sections. There are in fact other data that enable us to make the choice between the two structures and thereby to prefer the BLM(H)$-$Fe$^{III}-$OOH$^+$ (Figure 3d) form as the chemically more appropriate one. Thus, a protonated NH(A$_\beta$) group is more consistent with experiment (the Co^{III} complex in Figure 3a).[57] Moreover, analysis of structural data of BLM$-$Co^{III} published by Lehmann and Que (PDB code 1DEY)[55] revealed that their structure also has the same nitrogen protonated. This analysis indicates that protonation of NH(A$_\beta$), which takes place before formation of the activated form, is an inherent part of the structure, at least in solution. Indeed, starting with BLM$-$Fe$^{III}-$H$_2$O$_2^+$ where the amide ligand, N(**A**$_\beta$), is unprotonated, one proton shifts spontaneously from the hydrogen peroxide toward the negatively charged N(**A**$_\beta$) site to form a protonated ligand, NH(**A**$_\beta$). The energy of the latter species was lower by 25.2/29.0 kcal/mol in the gas-phase/aqueous solution (see SI, Figure S9) relative to the initial BLM$-$Fe$^{III}-$H$_2$O$_2^{1+}$ complex, thus indicating that the N(**A**$_\beta$) site is highly basic and will be protonated even before the ABLM is formed. Our choice for the heterolytic cleavage must then start from a protonated BLM(H)$-$Fe^{III} resting state complex. For the sake of completeness, however, we also investigated the unprotonated system, which led to similar final conclusions; these data are summarized in the Supporting Information (see, e.g., Figure S20b).

2. Electronic Structure of the Perferryl Species, [BLM$-$Fe^{V}=O]$^+$. Since the focus of present work is on mechanisms involving heterolytic O$-$O bond cleavage, we initially investigated the oxo$-$iron species, which are the products of heterolytic cleavage. In order to sort out the key factors of the electronic structure we generated Cpd I structures for both ^{2}BLM$-$Fe$^{III}-$OOH and ^{2}BLM(H)$-$Fe$^{III}-$OOH$^+$ complexes (Figure 3c and 3d). The results are shown in Figure 4a and 4b; for the latter Cpd I species, we considered an isomer that possesses NH(**A**$_\alpha$) and NH(**amide**) ligands and is shown in Figure 4c. By analogy with the heme-based complexes, here too the high-spin ($S = 3/2$) and low-spin ($S = 1/2$) states were investigated and found to be virtually degenerate. As expected, iron cannot easily sustain the Fe^V oxidation state,[61] and consequently, the complexes possess a triplet Fe^{IV}=O moiety ferromagnetically or antiferromagnetically coupled to an additional radical species located on one of the side moieties of BLM (BLM(H)), depending on the protonation state of the amide groups. In the case of the model in Figure 4a, the spin density of the third unpaired electron is localized mostly on the deprotonated amide group labeled as N(**A**$_\beta$), i.e., ^{2,4}[BLM$-$Fe^{IV}=O;N(**A**$_\beta$)$^\bullet]^+$. By contrast, when this amide group is protonated, i.e., NH(**A**$_\beta$) as in Figure 4b, the third unpaired electron is now delocalized over the linker region in the amidic moiety of the group **V**, i.e.,^{2,4}[BLM(H)$-$Fe^{IV}=O;**V**$^{\bullet+}]^{2+}$. Finally, in Figure 4c we show the doublet state of the isomer of the species in Figure 4b, where now the deprotonated ligand is the axial NH(**A**$_\alpha$) group for which the entire spin is located on this axial ligand, i.e.,^{2,4}[BLM(H)$-$Fe^{IV}=O;NH(**A**$_\alpha$)$^\bullet]^{2+}$. However, the latter isomer turns out to be much less stable than the one in Figure 4b, by 22.5/24.1 kcal/mol in the gas-phase/aqueous solution, respectively. Thus, the protonation state of the amide ligand has a profound effect on the electronic structure of the Cpd I species.

3. Electronic Structure of the BLM$-$Fe^{IV}=O Species. We also investigated the structural and electronic properties of the one-electron-reduced BLM$-$Fe^{IV}=O and BLM(H)$-$Fe^{IV}=O^{1+} species (see SI, Figure S7). Thus, upon reduction of the [BLM$-$Fe^{IV}=O; N(A$_\alpha$)$^\bullet]^{1+}$ and [BLM(H)- Fe^{IV}=O; V$^{\bullet+}]^{2+}$ species, the holes on the side chains get filled and the reduced species become analogous to Compound II (Cpd II) in heme and the non-heme oxidant systems.[15]

4. Energetic Aspects of the Heterolytic O$-$O Bond Cleavage. Heterolytic cleavage of the O$-$O bond that formally leads to the Cpd I type Fe^V=O species and H$_2$O is common in heme[4,36$-$38] and non-heme[2,12$-$14] biomimetic complexes. Some experimental findings suggest the presence of such a species also in bleomycin.[32,33] However, as noted there are also

(60) Kozlowski, P. M.; Nazarenko, V. V.; Jarzecki, A. A. *Inorg. Chem.* **2006**, *45*, 1424$-$1426.

(61) Ogliaro, F.; de Visser, S. P.; Groves, J. T.; Shaik, S. *Angew. Chem., Int. Ed.* **2001**, *40*, 2874$-$2878.

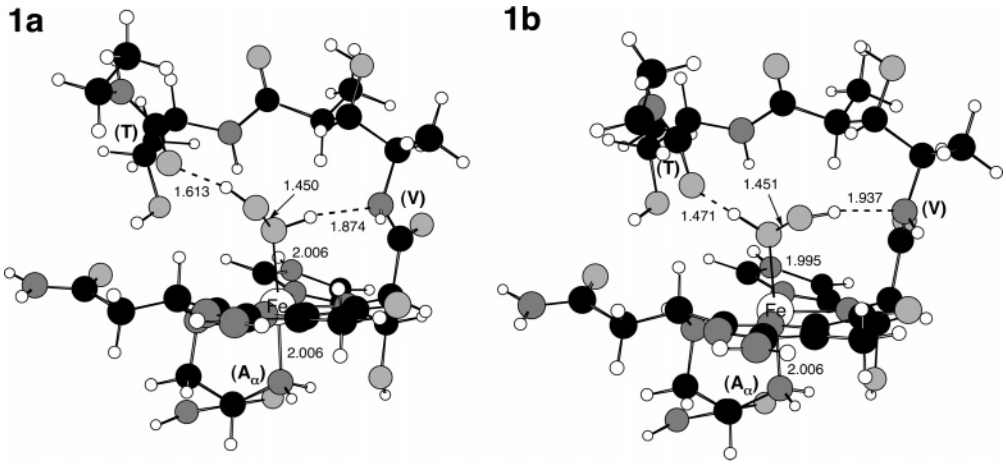

Figure 5. Optimized structures of the ^{2}BLM(H)−Fe^{III}−$(H_2O_2)^{2+}$ complexes **1a** and **1b** used for study of O−O heterolysis in Figures 6 and 7.

arguments against this proposal.[25−27,62] Briefly repeated, the main arguments are the following: (a) The presence of the Fe^V═O in heme proteins is stabilized by oxidation of porphyrin macrocycle (Por), resulting in a [(Por$^•$)Fe^{IV}═O]$^+$ Cpd I species, whereas in ABLM the ligands are much harder to oxidize, and (b) the heterolytic cleavage of the O−O bond should be energetically unfavorable due to the high solvation energy of the proton that is required for the bond heterolysis. Thus, using a "solvated proton" as the acidic source, heterolytic cleavage of the O−O bond in ABLM was estimated to be endothermic by +78.5 kcal/mol, compared with exothermicity of −78.3 kcal/mol for P450.[25−27] These positive reaction energies have been recently revised[62] using solvated NH_4^+ or H^+(solv) as proton sources; the new values are 25 kcal/mol for H^+ (solv) and 26 kcal/mol for NH_4^+. However, a solvated proton or ammonium ion is not a very realistic acid model for exploring the heterolytic cleavage processes. In enzymes or large biomolecules like bleomycin, the proton sources are acidic residues and/or sequestered water molecules,[37,46−48,63] in which case the protons are at all times covalently bound and further stabilized by the environment. Furthermore, in the generation of ABLM from the resting state of BLM(H)−Fe^{III} and H_2O_2 there is no need for an "external" proton because H_2O_2 itself is the source of the proton. Since H_2O_2 is by itself a poor acid[48,64] it can be deprotonated only when it is bound to the ferric iron. Indeed, our preliminary tests showed that the intrinsic acidity of the hydrogen peroxide is very strongly enhanced by the formation of the Fe^{III}−H_2O_2 complexes (see SI, Table S1a). Therefore, protons should generally be available to the BLM when Fe^{III}−OOH is generated from the Fe^{III}−H_2O_2 complex. As such, what is left is to find out if the proton originating in H_2O_2 can be shuttled easily to cleave the O−O bond in a heterolytic manner.

To explore realistic heterolytic cleavage mechanisms, the ^{2}BLM(H)−Fe^{III}−$H_2O_2{}^{2+}$ complex was first generated from the corresponding ferric−hydroperoxide complex in Figure 3d. We assumed that the ^{2}BLM(H)−Fe^{III}−$H_2O_2{}^{2+}$ complex can be formed from the ferric resting state of BLM(H)−Fe^{III}. There is ambiguity about the nature of the ferric BLM(H)−Fe^{III} complex, whether it should be formulated as BLM−Fe^{III}−OH or BLM−Fe^{III}−OH_2. Sugiura[65] originally hypothesized that the resting ferric state is BLM−Fe^{III}−OH based on ESR spectroscopy, but he did not rule out the presence of the BLM−Fe^{III}−OH_2 complex (see p 5212). Subsequently, Takahashi et al.[66] confirmed the BLM−Fe^{III}−OH hypothesis using arguments based on low-frequency Fe−OH region and deuterium shifts; this assignment relied on indirect comparison of the resonance Raman spectrum of the ferric−BLM complex with simple ferrous−aqua complexes such as $[Fe^{II}(H_2O)_6]^{2+}$ or $[Zn(H_2O)_6]^{2+}$. Thus, it was argued that since in the latter complexes the Fe−O frequency was low (389 cm^{-1}) whereas in the resting state of BLM−Fe^{III} the frequency was much higher (561 cm^{-1}), it followed that the latter must be BLM−Fe^{III}−OH. However, recent studies by Spiro and co-workers[67] employing resonance Raman spectroscopy and DFT-based normal coordinate analysis showed that the Fe^{III}−OH_2 frequency is 523 cm^{-1} and hence is in fact much higher than the values assumed by Takahashi et al.[66] and used to rule out the BLM−Fe^{III}−OH_2 formulation. On the basis of Spiro's frequency data, the BLM−Fe^{III}−OH_2 form fits better and is a more consistent form of the resting state. In addition, as we argued above, the bleomycin ligand is the BLM(H)$^{1-}$, protonated at the N(A_β) site. Since H_2O is an easily replaceable ligand, the Fe^{III}−H_2O_2 complex can in fact be formed and generate ABLM by losing a proton to the side chains of the BLM; it shall be seen that the proton shift is thermoneutral or slightly exothermic. Accordingly, the heterolytic cleavage mechanisms were studied using the ^{2}BLM(H)−Fe^{III}−$(H_2O_2)^{2+}$ complex as described below (the corresponding data for ^{2}BLM−Fe^{III}$(H_2O_2)^{1+}$ is given in the Supporting Information; see, e.g., Figure S20b).

Figure 5 shows the optimized structures of the two most stable conformations, **1a** and **1b**, which were used for the heterolytic study since they are the ones set up for proton reshuffle. Inspection of the optimized structures of these Fe^{III}−H_2O_2 complexes demonstrates that the hydrogen peroxide moiety is clamped by hydrogen bonds with the NH(**V**) and C═O(**T**) groups (see also the ^{2}BLM(H)−Co^{III}−OOH$^+$, ^{2}BLM−Fe^{III}−OOH, and ^{2}BLM(H)−Fe^{III}−OOH$^+$ structures in Figure 3a, c, and d). As such, this hydrogen-bonding network can serve as

(62) Decker, A.; Chow, M. S.; Kemsley, J. N.; Lehnert, N.; Solomon, E. I. *J. Am. Chem. Soc.* **2006**, *128*, 4719−4733.
(63) Harris, D. L. *J. Inorg. Biochem.* **2002**, *91*, 568−585.
(64) Jones, P.; Dunford, H. B. *J. Inorg. Biochem.* **2005**, *99*, 2292−2298.
(65) Sugiura, Y. *J. Am. Chem. Soc.* **1980**, *102*, 5208−5215.
(66) Takahashi, S.; Sam, J. W.; Peisach, J.; Rousseau, D. L. *J. Am. Chem. Soc.* **1994**, *116*, 4408−4413.
(67) Jarzecki, A. A.; Anbar, A. D.; Spiro, T. G. *J. Phys. Chem. A* **2004**, *108*, 2726−2732.

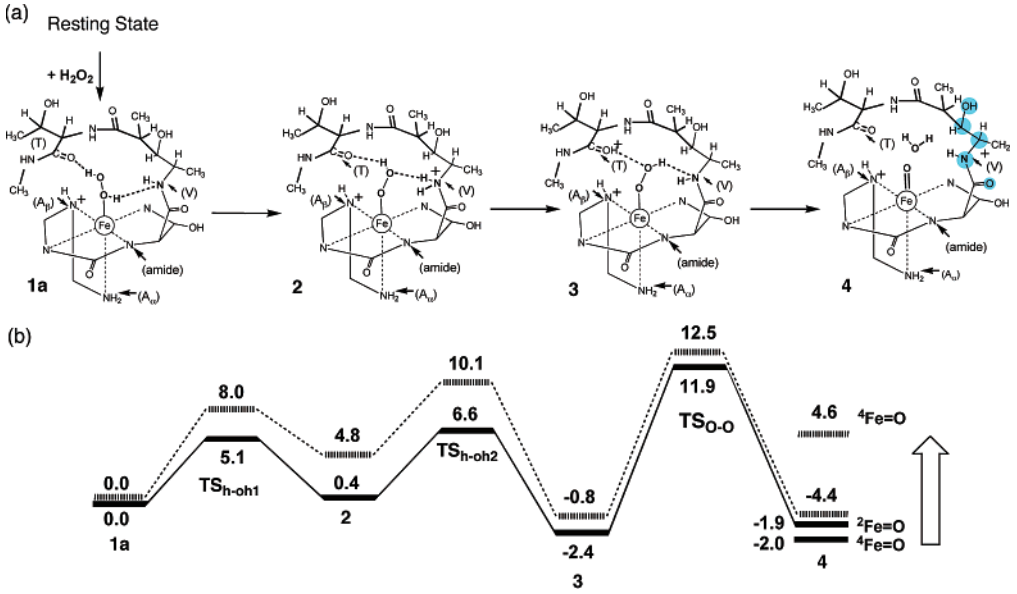

Figure 6. (a) Schematic representation of proton reshuffle heterolytic cleavage of the O−O bond of BLM(H)−$Fe^{III}(H_2O_2)^{2+}$, **1a**, initiated by the NH(V) group. (b) The corresponding UB3LYP/B2//B1 energy profiles. The dashed lines represent relative energies of the corresponding species in aqueous solution (i.e., UB3LYP/B2+solvent//B1). For detailed geometries of the structures, see other figures: **1a** in Figure 5 and **2**−**4** and TSs in Figure 8.

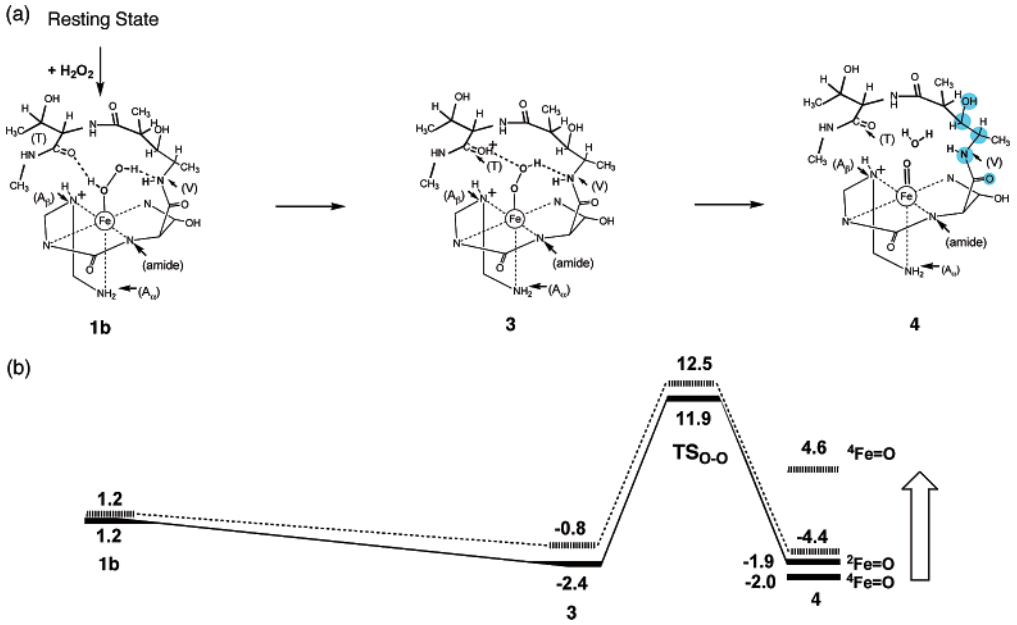

Figure 7. (a) Schematic representation of proton reshuffle heterolytic cleavage of the O−O bond in the BLM(H)−$Fe^{III}(H_2O_2)^{2+}$ conformer, **1b**, mediated by the C═O(T) group. (b) The corresponding UB3LYP/B2//B1 energy profiles. The dashed lines represent relative energies of the corresponding species in aqueous solution (i.e., UB3LYP/B2+solvent//B1). For detailed geometries of the structures, see other figures: **1b** in Figure 5 and others in Figure 8.

conduit of proton reshuffle that will convert the $Fe^{III}-H_2O_2$ to a Cpd I like Fe^{V}═O species in a manner similar to the Poulos−Kraut mechanism in heme peroxidases.[46,47] We cannot rule out that a water molecule(s) can enter the cavity and help mediate the process or generate Fe^{V}═O species analogous to those suggested in the non-heme Que reagents.[2,12,13] However, to avoid speculations about the water content and complicating an already complex system the role of water was not explored.

As anticipated, the BLM environment and coordination to Fe^{III} increase the acidity of H_2O_2. Indeed, Figure 5 reveals that the NH(**V**) and C═O(**T**) groups may easily deprotonate the proximal position of hydrogen peroxide in the $Fe^{III}-H_2O_2$ complexes and generate the corresponding ABLM Fe^{III}−OOH complexes. Accordingly, we studied the two possible O−O cleavage pathways initiated from these **1a** and **1b** complexes **(**another conformation, **1c**, in Figure S10, is virtually of the same stability but was not chosen since it is less prepared for the proton reshuffle). Initially, we calculated the gas-phase energy profiles and then corrected the energy of the species by solvation energies in aqueous solution. The scans, energy profiles, and structures for the processes nascent from the $Fe^{III}-H_2O_2^{2+}$ complexes are summarized in the Supporting Information (Figures S10−S19, Table S2).

The energy profiles for heterolytic cleavage starting from the BLM(H)−Fe−$H_2O_2^{2+}$ complexes, **1a**,**b** are shown in Figures 6 and 7; the solid lines correspond to the gas-phase calculations, while the dashed bars denote the solvation-corrected energies of the respective species. The detailed geometries **1a** and **1b**

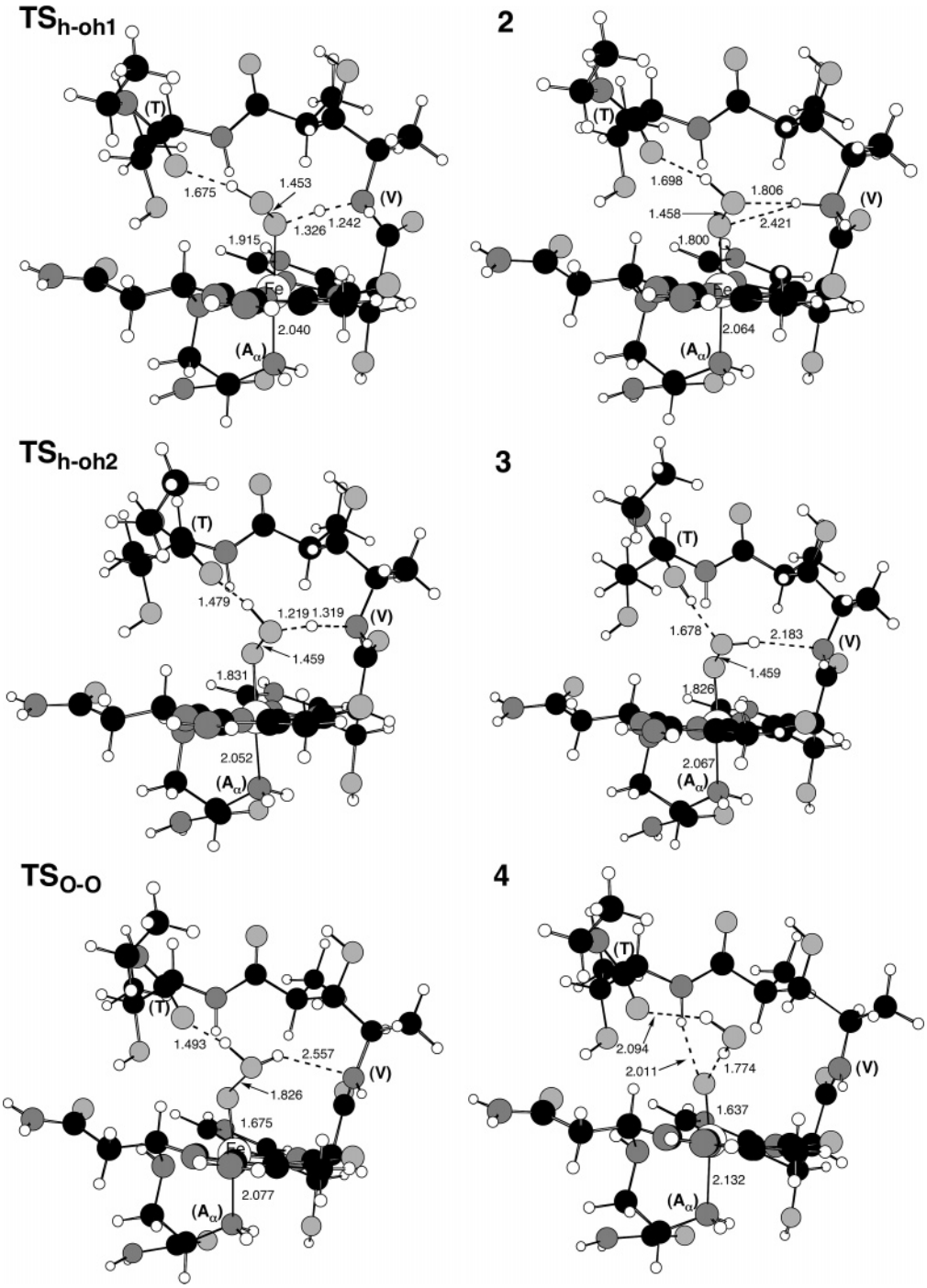

Figure 8. Structures of species **2**−**4** and the **TS**s corresponding to the profiles of Figures 6 and 7. Note that species **3**, **TS**$_{O-O}$, and **4** are common to the mechanisms in Figures 6 and 7.

are given above in Figure 5, while the remaining structures, **2**, **3**, and the various transition states (**TS**s), are depicted in Figure 8.

Figure 6 starts with the **1a** conformer of $Fe^{III}-H_2O_2^{2+}$ which undergoes proximal deprotonation by NH(**V**) to yield the $Fe^{III}-OOH$ complex, **2**, via the transition-state species, **TS**$_{h-oh1}$. Subsequently, the NH_2^+(**V**) group relays a proton back to the distal oxygen, which simultaneously loses a proton to the C═O(**T**) group, via **TS**$_{h-oh2}$, to form **3**, a conformer of $Fe^{III}-OOH$ with a protonated C═OH^+(**T**) side group. Starting from the latter complex, the C═OH^+(**T**) group transfers a proton to the distal oxygen of the $Fe^{III}-OOH$ complex and leads thereby to heterolytic O−O cleavage, departure of a water molecule, and formation of the Cpd I like species, **4** (see electronic structure in Figure 4b). The last step via **TS**$_{O-O}$ (imaginary frequency of TS_{O-O}; 477*i* cm^{-1}) is the rate-determining step of this mechanism. Unlike in P450,[68] here we could not locate a stable BLM-(H)−Fe−OOH_2^{2+} intermediate. However, in accord with the most recent findings on the heterolytic cleavage mechanism in P450 based on QM/MM and large QM-model calculations,[68]

(68) (a) Kumar, D.; Hirao, H.; de Visser, S. P.; Zheng, J.; Wang, D.; Thiel, W.; Shaik, S. *J. Phys. Chem. B* **2005**, *109*, 19946−19951. (b) Zheng, J.; Wang, D.; Thiel, W.; Shaik, S. *J. Am. Chem. Soc.* **2006**, *128*, 13204−13215.

here too the process from Fe−OOH to the Cpd I species is virtually thermoneutral.

Figure 7 depicts the energy profile when the C═O(**T**) moiety acts as a base that abstracts the proximal proton of H_2O_2 from **1b**. The scan for this process shows a barrier of less than 1 kcal/mol (Figure S19c), and therefore, deprotonation is virtually barrierless, leading to the Fe^{III}−OOH complex **3** (see Figure 8). Compared with Figure 6, deprotonation of the hydrogen peroxide by C═O(**T**) is slightly exothermic and reminiscent of the recent value computed by QM/MM for horseradish peroxidase.[48] From **3** onward the mechanism is identical to Figure 6, and formation of Cpd I (**4**) occurs via $\mathbf{TS}_{O-O}$. With solvation correction, the barrier in Figure 7 is 13.3 kcal/mol.

In summary, Figures 6 and 7 show that when the proton source is a coordinated H_2O_2 molecule and the base is a group in the cavity of the BLM, the proton reshuffle is facile and O−O cleavage is the rate-determining step for formation of the perferryl species, **4**, via either mechanism. Despite the slightly higher energy of **1b** vs **1a**, these species are almost equally stable, and since the mechanism in Figure 7 is direct and less complex than in Figure 6, this is our preferred choice. This preference is however not essential since in the end the two mechanism are very similar with the same rate-controlling step, via $\mathbf{TS}_{O-O}$. The highest barrier for each of these mechanisms is 13.3 kcal/mol. For comparison, the analogous mechanism to Figure 7, but with the unprotonated N($\mathbf{A}_\beta$) site, gave a highest barrier of 10.9 kcal/mol (see Figure S20b; B2 datum with solvent corrections).

5. Comparison with Other Modes of O−O Bond Cleavage. Let us start with a brief assessment of the just outlined heterolytic cleavage vis-à-vis a potential homolytic cleavage of the O−O bond (Figure 2). Thus, while the mechanisms in Figures 6 and 7 lead to formation of Cpd I that can subsequently abstract a hydrogen from DNA, the O−O homolysis will lead to formation of a Fe^{IV}═O Cpd II species and a free HO$^\bullet$ radical that may, in turn, cause DNA cleavage via hydrogen abstraction. The homolytic O−O bond dissociation energies were estimated for the BLM−Fe^{III}−OOH and BLM(H)−Fe^{III}−OOH^+ models. The corresponding values are the following (the values were not corrected for ZPVE, BSSE, or solvent effects)

$$^2\text{BLM}-\text{Fe}^{III}-\text{OOH} \rightarrow {}^3\text{BLM}-\text{Fe}^{IV}=\text{O} + {}^2\text{OH}^\bullet \qquad (\Delta E = 32.0 \text{ kcal/mol})$$

$$^2\text{BLM(H)}-\text{Fe}^{III}-\text{OOH}^+ \rightarrow {}^3\text{BLM(H)}-\text{Fe}^{IV}=\text{O}^+ + {}^2\text{OH}^\bullet \qquad (\Delta E = 31.2 \text{ kcal/mol})$$

As one could have expected, the protonation states of the amide groups have a negligible influence on the O−O bond dissociation energy. The possibility that other spin states, except for the triplet states of BLM−Fe^{IV}═O^0 and BLM(H)−Fe^{IV}═O^+ (Figure S7), could be involved in the cleavage was also investigated and ruled out on energetic grounds. The above energy estimates using realistic structural models of Fe^{III}−OOH ABLM are in agreement with value of 29 kcal/mol reported by Solomon and co-workers.[25,27] These values for the homolytic cleavage are significantly higher than the barriers for the heterolytic cleavage of Fe^{III}−OOH (Figures 6 and 7). Of course, the transition state of the homolytic cleavage mechanism would be lower than the bond dissociation energy limit, and by analogy to heme systems may be estimated as 18−21 kcal/mol.[39d]

Another alternative mechanism whereby the Fe^{III}−OOH ABLM can directly participate in DNA cleavage is by direct H abstraction from the sugar moiety of DNA (Figure 2).[27] Our attempts to locate a transition state for direct H abstraction ended in a structure that had an essentially cleaved O−O bond and an OH radical that performed the H abstraction (see Supporting Information for details). When our manuscript was under preparation a computational study of a mechanism of direct H abstraction was published.[62] However, inspection of the published transition state reveals an unusually long O−O bond of 2.7 Å and a very low imaginary frequency (195*i* cm^{-1}), implying that the O−O bond is already cleaved in the reported transition state, and one may wonder if this is indeed a direct H-abstraction mechanism or a mechanism involving initial O−O bond homolysis, as suggested by Sligar et al.[31] However, such a mechanistic assignment would require IRC calculation. Importantly, the best estimate for the activation energy of this direct process was 18/17 kcal/mol for the gas-phase/solvent environment with ZPVE correction, respectively.[62] The values are higher by about 4−5 kcal/mol than energy barriers for the heterolytic cleavage.

Discussion

This study used DFT/UB3LYP calculations to explore the mechanism of O−O bond activation, starting with the BLM-(H)Fe^{III}−H_2O_2 complex of a realistic structural model of bleomycin. Two alternative mechanisms were located and are shown in Figures 6 and 7. The mechanism involves acid−base proton reshuffle mediated by the side-chain linkers of BLM in a manner akin to the mechanism in peroxidases.[46−48,64] Thus, in the mechanism in Figure 7 an initial deprotonation of hydrogen peroxide by the carbonyl moiety, C═O(**T**), of the threonine terminal linker leads to the C═OH^+(**T**)/Fe^{III}−OOH species, **3**. Subsequently, the C═OH^+(**T**) moiety relays the proton back to the distal oxygen atom of Fe^{III}−OOH and causes O−O heterolysis that generates a water molecule and the Cpd I like species. The so-formed Cpd I species, **4**, is a BLM−Fe^{IV}═O complex with a radical on the side-chain linker methylvalerate (**V**); see electronic structure in Figure 4b. The mechanism in Figure 6 is slightly more complex; it involves an initial proton transfer from Fe−H_2O_2 to the NH(**V**) side group to form the NH_2^+(**V**)/Fe^{III}−OOH complex **2**, which then shuttles the proton C═O(**T**) with subsequent O−O cleavage to give the same Cpd I species, BLM−Fe^{IV}═O; $\mathbf{V}^{+\bullet}$. The two mechanisms of formation of Cpd I are found to involve a barrier of 13.3 kcal/mol and are energetically feasible, certainly no less feasible than the other alternative mechanisms, homolytic cleavage and/or direct H abstraction[62] by ABLM (in Figure 2). Furthermore, in Figures 6 and 7, the rate-determining step of the heterolytic cleavage is the O−O bond via $\mathbf{TS}_{O-O}$. This result may explain the KIE(^{18}O) data observed[29] during the decay of ABLM and the finding that the rate of this decay was not affected by DNA. Such an observation would fit a scenario whereby Fe^{III}−OOH undergoes O−O bond heterolysis, unaffected by DNA, and forms an active species that subsequently cleaves DNA.

In this respect, the analogy of the heterolytic mechanism in Figures 6 and 7 to the Poulos−Kraut mechanism in the catalytic cycle of heme peroxidases[46] extends to the electronic structure of the Cpd I like species. Thus, the resulting Cpd I intermediate has two unpaired electrons located on the Fe═O unit and an additional one delocalized over the **V** linker region, i.e., the

$[BLM(H)-Fe^{IV}=O;\mathbf{V}^{\bullet+}]^{2+}$ species (**4** in Figures 4b and 6−8). This structure of the Cpd I species is analogous to the species in cytochrome *c* peroxidase (C*c*P)[47] that possesses a triplet $Fe^{IV}=O$ moiety and an additional unpaired electron in the neighboring amino acid residue, tryptophan. While an analysis of the reaction associated with DNA cleavage is beyond the scope of present work, one may further extend the analogy with C*c*P and suggest that the oxidized $\mathbf{V}^{\bullet+}$ linker of $[BLM(H)-Fe^{IV}=O;V^{\bullet+}]^{2+}$ may play a similar role to the tryptophan radical cation in the active species of C*c*P, namely, to abstract an electron/H^+ or a hydrogen from DNA as a primary event of its cleavage.

In both heterolytic mechanisms there is no need for an "external" proton; the proton "arrives" with the hydrogen peroxide ligand and is re-shuttled quite easily within the BLM cavity, passing via protonated $BLM(H)Fe^{III}$−hydroperoxo complexes **2** and **3**, and leading eventually to heterolytic O−O cleavage via $\mathbf{TS}_{O-O}$. The proton in transit is bonded and engaged also in strong hydrogen bonding throughout the process; it will therefore not be spontaneously lost to the exterior of the BLM. Thus, as long as the proton is inside the BLM, the Cpd I species will be formed easily. Loss of the proton, e.g., from **3** to a water molecule (however, $pK_a(H_3O^+) = -1.74$) in the exterior of BLM will lead to the proton-free low-spin $BLM(H)Fe^{III}$−hydroperoxo complex (Figure 3d). As such, the two species, Cpd I and BLM(H)Fe−OOH may coexist rather than being mutually exclusive. To obtain a proper assessment of the proton loss to the exterior of BLM (or vice versa from outside in) the process will have to be studied by QM/MM calculations of BLM in the native environment (presumably aqueous) with a QM subsystem that also includes a sufficiently saturated water cluster and with sampling to account for the free energy of the process. Simple estimates of protonation energy differences between separated species (H^+, H_3O^+, NH_4^+, etc.) can lead to large errors as found in the heterolytic cleavage studies in P450.[68]

In fact, the available experimental observations do not rule out at this point any mechanism in a definitive manner. Thus, the recent observation[62] of a kinetic solvent isotope effect, KSIE (H_2O/D_2O), of 3.6 on the decay of ABLM can fit a water-assisted heterolytic cleavage mechanism of BLM(H)Fe−OOH (followed by further consumption of Cpd I). The observation of KSIE just tells that there is some shuttling of protons via water to the reaction center. However, the precise value of KSIE (H_2O/D_2O) cannot actually distinguish the mechanisms, at least not in a definitive manner. Thus, in P450cam[69] a KSIE value of 1.8 was reported for heterolytic O−O cleavage in the wild-type (WT) enzyme, whereas for the same process in the Asp251Asn mutant the value reached 10! The difference between the values arose due to the fact that in the WT enzyme a water molecule is shuttling a proton from a strong acid like Asp while the proton shuttle involved only a cluster of water molecules. Similarly, computations of KSIE for the decay of the Fe^{III}−OOH species of heme oxygenase[70] via a homolytic dissociation mechanism gave variable results (1.3−4.7) depending on the acidic source of the proton. Finally, the observation that hydrogen-atom donors like ascorbic acid and 4-hydroxy-TEMPO-H[62] caused ABLM to decay with a KIE(H/D) of 3 is interesting since ascorbic acid is a well-known peroxidase substrate as are various phenols.[46,71] These molecules react with Cpd I of peroxidases by a proton-coupled electron-transfer (PCET) process,[71] and while the molecules may react also with ABLM in a direct hydrogen abstraction process,[62] the observation of KIE is not a proof that the latter is the only possible mechanism for ABLM. A PCET mechanism with Cpd I is a viable alternative. Decker and Solomon[62] calculated the H-abstraction reactivity of the BLM−Cpd II species (obtained by OO homolysis from ABLM) toward a sugar model and found a barrier of 12 kcal/mol. Considering that generally Cpd I species are more reactive than Cpd II,[4,36−38] at least in the heme species one would expect the BLM−Cpd I species to have a barrier somewhat lower than 12 kcal/mol. There are many interesting mechanistic features that need to be explored regarding the reactivity of Cpd I with DNA and substrates like ascorbate and 4-hydroxy-TEMPO-H; one of these is the PCET mechanism analogous to peroxidases, where in addition to the Fe(IV)=O moiety, a role is played also by the radical center on $\mathbf{V}^{+\bullet}$. This study is however well beyond the scope of the present paper.

Conclusions

The DFT calculations discussed above present an alternative hypothesis to the exclusive reactivity of the Fe^{III}−OOH species of bleomycin (BLM), so-called activated BLM (ABLM). The calculations show that if one starts with $BLM(H)Fe^{III}-H_2O_2$ there is a very facile proton shuttle mechanism mediated by the side-chain linkers of BLM that abstract the proximal proton of the hydrogen peroxide and relay it to the distal oxygen with simultaneous departure of a water molecule and formation of a Compound I (Cpd I) type species (Figures 6 and 7) in a manner akin to the mechanism in peroxidases.[46−48,64] The Cpd I species involves a $BLM(H)-Fe^{IV}=O$ and a $\mathbf{V}^{+\bullet}$ radical species in the side-chain linker methylvalerate (Figure 1). Formation of Cpd I is found to involve a barrier of 13.3 kcal/mol, which in turn means that the cleavage reaction would be fast. We therefore suggest that Cpd I of BLM may participate in DNA cleavage. Experimental data of various kinetic isotope effects[29,62] are discussed and shown to fit also Cpd I reactivity.

The new mechanisms may be probed by experimental strategies that mutate the groups participating in the proton reshuffle in a manner that will reveal whether the **V** and CO-(**T**) groups have indeed some unique role in activating BLM and/or DNA cleavage. Studies with such mutated BLMs are known,[21,72,73] but their connection with the proton-shuffle mechanism presented here is not straightforward and will require future elucidation. On the basis of studies of model systems, which perform DNA cleavage satisfactorily, one may argue that the side-chain linker is not essential to the BLM action. This however does not prove that BLM acts in the same manner as model systems (for which there may well be alternative modes of generating a Cpd I or Cpd II species like in non-heme sytems[2]); the importance of mutations should be tested on BLM itself and not by comparison to model systems.

Finally, as we already argued, ABLM and BLM−Cpd I are not necessarily mutually exclusive, and there may be additional

(69) Vidakovic, M.; Sligar, S. G.; Li, H.; Poulos, T. L. *Biochemistry*, **1998**, *37*, 9211−9219.
(70) Kumar, D.; de Visser, S. P.; Shaik, S. *J. Am. Chem. Soc.* **2005**, *127*, 8204−8213.
(71) Henriksen, A.; Smith, A. T.; Gajhede, M. *J. Biol. Chem.* **1999**, *274*, 35005−35011.
(72) Boger, D. L.; Ramsey, T. M.; Cai, H.; Hoehn, S. T.; Stubbe, J. *J. Am. Chem. Soc.* **1998**, *120*, 9139−9148.
(73) Boger, D. L.; Ramsey, T. M.; Cai, H.; Hoehn, S. T.; Stubbe, J. *J. Am. Chem. Soc.* **1998**, *120*, 9149−9158.

mechanisms that lead to BLM−Cpd I. One of these mechanisms, which will have to be considered in the future, is the heterolytic O−O cleavage induced by a molecule of water that may coordinate to the iron and lead to a HO−Fe^{V}═O species in a manner akin to non-heme systems.[2,12−14] There may be other articulations of the idea such that the alternative hypothesis of BLM Cpd I species can re-open the field and form a basis for the interplay of experiment and theory.

Acknowledgment. The Hebrew University group is supported by a DIP grant from BMBF-DIP (grant no. DIP-G.7.1), while P.M.K. is supported by the National Institute of Health (COBRE grant RR018733). The sabbatical stay of P.M.K. at the Hebrew University was supported by The Fulbright Foundation and in part by the Lise Meitner-Minerva Center for Computational Quantum Chemistry.

Supporting Information Available: Twenty-one figures, two tables, and *XYZ* coordinates (PDF). This material is available free of charge via the Internet at http://pubs.acs.org.

JA064611O